Zeeman Splitting

Sam Silva
December 2019

Abstract: By placing a mercury lamp inside a magnetic field, one can observe the Zeeman effect where the mercury atoms interact with the magnetic field and undergo energy transitions. These transitions allow for calculation of the physical constant, the Bohr magneton. In this lab the Bohr magneton was found to be $8.616 \times 10^{-24} \pm 8.7 \times 10^{-27}$ J/T, $9.258 \times 10^{-24} \pm 9.07 \times 10^{-27}$ J/T, $8.908 \times 10^{-24} \pm 8.9 \times 10^{-27}$ J/T, for 3, 6, and 9 energy transitions, respectively.

Introduction

When atoms are located in a magnetic field they undergo spectral splitting, dubbed as the Zeeman effect. Important applications of the Zeeman effect are included in quantum mechanics and the fields of nuclear magnetic resonance spectroscopy, electron spin resonance spectroscopy, and magnetic resonance imaging. By utilizing interferometry techniques as well as data extraction methods, one can understand the fundamental principals of Zeeman splitting through numerical and visual analyses. A mercury lamp is placed in a magnetic field where a camera is used to pick up the spectral lines. Through the analysis of the radii, one can solve for the Bohr magneton which represents the fundamental unit of angular momentum, e.

Theory

The Zeeman effect was discovered by Pieter Zeeman when he placed a sodium light in a strong magnetic field and observed how the lines would broaden. For this experiment a mercury lamp is used. The principals behind the Zeeman effect can be explained through quantum mechanics.

Level Splitting

Level splitting occurred when the atoms were in the presence of a magnetic field, where the spectral lines would split into several more lines. When observing the spectral lines through the camera, three rings coincided within wider rings became distinguishable. The rings occurred as the mercury exhibited a transition from the 3S1(6s7s) energy level to the 3P2(6s6p) level. Based on the notation of (6s7s), it is inferred that mercury has two valence electrons with one belonging to the 6s orbital and the other to the 7s orbital. The orbital angular momentum quantum number for an S state is $L = 0$ and for a P state is $L = 1$. Since mercury has two valence electrons, they are paired to form a spin quantum number, $S = 1$. This results is the total momentum quantum numbers for the states of $J = 1$ and $J = 2$, respectively. When the atoms are in the presence of a magnetic field, each energy level splits into $2J + 1$. Figure 1 depicts the splitting, where the lines are spaced not to scale, but the splitting is than 10^{-5}.

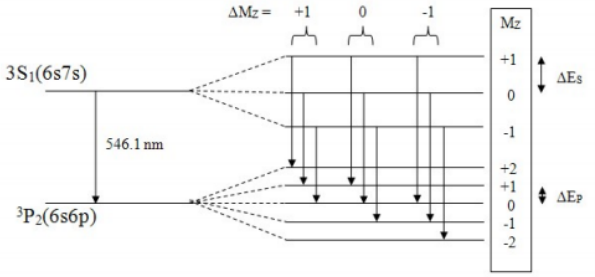

Figure 1: The energy levels of the green line in mercury. The levels without a magnetic field are on the left and with a magnetic field are on the right.

Based on electromagnetic selection rules for quantum states, the transition states are between $\Delta M_Z = +1, 0, -1$, where the transition lines from $\Delta M_Z = 0$ are the most intense. Using Figure 1 as reference, E_s is the energy of the "un-split" 3S1 state which has a magnetic field (B) of zero. This is equal to the $M_Z = 0$ energy level when the field is non-zero. ΔE_S is the shift energy from the S state when the magnetic field is non-zero. The P energy states are defined in the same fashion. The energy shift is determined by the component of the magnetic moment of the atom along the magnetic field and is represented by

$$\Delta E = M_Z g_L B \mu_B, \tag{1}$$

where μ_B is the Bohr Magnetron and g_L is the Lande g factor. The Bohr magnetron is the classical magnetic moment that an electron in the first Bohr orbit of hydrogen would have. This electron can be treated as if it is a tiny current loop with current

$$i = \frac{e}{T} = \frac{eh}{m(2\pi r_B)^2} \tag{2}$$

where T represents the time for one orbit of the electron, v is the speed of the electron in the first Bohr orbit, m is the electron mass, and r_B is the Bohr radius. The magnetic moment of a single current loop is

$$\mu_B = iA = i(\pi r_B^2) = \frac{eh}{4\pi m} = 9.274 \times 10^{-24}\,\text{J/T} \tag{3}$$

where A is the area of the loop. Since this derivation uses classical mechanic principals for the Bohr orbits, the first Bohr orbit of hydrogen is incorrect, however, the Bohr magnetron is still correct. The Lande g factor is defined as

$$g_L = 1 + \frac{J(J+1) + S(S+1) - L(L+1)}{2J(J+1)}. \tag{4}$$

Using Equation 4, one can solve for the Lande g factors for the S and P states of mercury. For the S state: $L = 0$, $S = 1$, and $J = 1$, which resulted in $g_S = 2$. For the P state: $L = 1$, $S = 1$, $J = 2$, which resulted in a $g_P = 3/2$

When $B = 0$, a transition from the S to the P state results in a photon with a frequency V_0 given by

$$hv_0 = E_S - E_P. \tag{5}$$

However, when there is a magnetic field, the frequency v of an emitted photon is

$$hv = (E_S + \Delta E_S) - (E_P + \Delta E_P) = hv_0 + (\Delta E_S + \Delta E_P) \tag{6}$$

Substituting in Equation 1 provides

$$v = v_0 + (M_{zi} g_S - M_{zf} g_P)\frac{B\mu_B}{h}, \tag{7}$$

where M_{zi} and M_{zf} are the initial and final values of M_z, respectively. The frequency is expressed as

$$v = v_0 + \delta\frac{B\mu_B}{h} \tag{8}$$

where δ is defined as

$$\delta = M_{zi} g_s - M_{zf} g_p. \tag{9}$$

Using Equation 9, substitute in the Lande g factor that was found earlier. The resulting δs can be found in Table 1.

Table 1: δ for each energy transition for mercury.

Energy Transistions	δ
$+1 \rightarrow +2$	-1
$0 \rightarrow +1$	-3/2
$-1 \rightarrow 0$	-2
$+1 \rightarrow +1$	1/2
$0 \rightarrow 0$	0
$-1 \rightarrow -1$	-1/2
$+1 \rightarrow 0$	2
$0 \rightarrow -1$	3/2
$-1 \rightarrow -2$	1

Fabry-Perot Interferometer

A Fabry-Perot interferometer is used to make a good measurement of small differences in frequency. The interferometer is made up of two partially reflective mirrors that are spaced at distance d. There is also a collimating lens which causes rays of light that originate on the optical axis to come in parallel to the optical axis. However,the source is not a point source and rays that originate on the source at a position that is at a small angle, θ, from the optical axis seen from the collimating lens will reach the interferometer nearly parallel and at the same angle θ from the optical axis as shown in Figure 2. Ray 1 will be partially reflected at points A and B. It then interferes with ray 2 because both rays follow the same path after point B. Ray 1 travels along a path that is longer than ray 2 by

$$\Delta l = 2dcos(\theta). \tag{10}$$

Constructive interference will occur when

$$\Delta l = 2dcos(\theta) = n\lambda \tag{11}$$

where λ is the wavelength and n is an integer. Because θ is extremely small, we can keep two terms in the Taylor series approximation,

$$cos(\theta) = 1 - \frac{\theta^2}{2!} + ... \tag{12}$$

Using this approximation, Equation 11 became

$$n = \frac{2d}{\lambda}(1 - \theta^2/2), \tag{13}$$

where n_0 is defined as

$$n_0 \equiv \frac{2d}{\lambda}. \tag{14}$$

For constructive interference to occur, n must be an integer, however, n_0 does not need to be an integer. Write n_0 as the number of wavelengths that fit in a distance 2d. If n_0 was an integer, then there would be constructive interference at the center ($\theta = 0$), but in this case it is not.

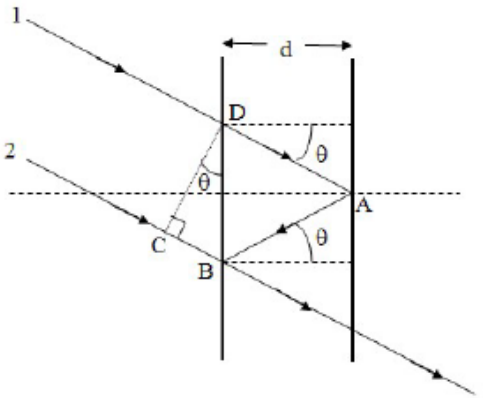

Figure 2: Geometry of the Fabry-Perot interferometer.

The light exiting the interferometer at an angle θ_k os focused by a lens to form the k^{th} ring with a radius of R_k on the detector plane of a camera. The geometry of the formation of a ring is shown in Figure 3. Since the angle is small, it is related to the radius by

$$\theta_k \approx \frac{R_k}{f}, \tag{15}$$

where f is the focal length. The focal length of the camera lens is adjustable, but it is kept fixed once the rings are in focus.

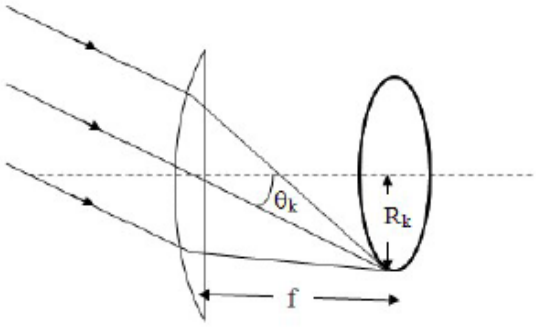

Figure 3: Geometry of the formation of a ring on the detector of the camera.

Based on Equations 11 and 14, we get

$$n = n_0 cos(\theta) \tag{16}$$

If n_1 is the interference order of the first ring, then $n_1 < n_0$. Let

$$n_1 = n_0 - \epsilon \tag{17}$$

The k^{th} ring of the pattern measured from the center outwards is in the order of

$$n_k = (n_0 - \epsilon) - (k - 1) \tag{18}$$

Combining equations 13, 15, and 18 yields

$$R_k^2 = \frac{2f^2}{n_0}(k - 1 + \epsilon) \tag{19}$$

Assuming the radii of rings associated with the same wavelength, then a plot of R_k^2 vs. k should be a straight line. Extrapolating back to R_k^2, which is closely spaced. From using equations 14 and 17, one gets

$$\frac{2d}{\lambda_a} = n_{1a} + \epsilon_a. \tag{20}$$

Since the frequencies can be written as $v_a = c/\lambda_a$ and $v_b = c/\lambda_b$, then one can rewrite Equation 20 as

$$\frac{2d}{c}(v_a - v_b) = (\epsilon_a - \epsilon_b). \tag{21}$$

Substituting Equation 8 into Equation 22 becomes

$$\frac{2dB\mu_B}{hc}(\delta_a - \delta_b) = \epsilon_a - \epsilon_b, \tag{22}$$

which suggests that a plot of ϵ vs. δ should be linear. Extracting the slope from the best fit can be used to find the Bohr magneton.

Solving for the Bohr Magneton

The Bohr magneton is a physical constant and the natural unit for expressing the magnetic moment of an electron caused by either its orbital or spin angular momentum. Using Equation 22, it is possible to extract the Bohr magneton, μ_B, when ϵ vs. δ is plotted. The plot of vs. δ yields a slope,

$$\frac{2dB\mu_B}{hc}, \tag{23}$$

where d is the distance between the reflective mirrors in the Fabry Perot interferometer. Its value is 0.00195 $\pm$ 2×10^{-6} m. Planck's constant times the speed of light is denoted as hc, and B is the value of the magnetic field at 5 Amps. The Bohr magneton can be written as

$$\mu_B = \frac{m * hc}{2dB}, \tag{24}$$

with m being the slope of ϵ vs. δ. To find ϵ use Equation 19, which can be rewritten as

$$R^2 = \frac{2f^2}{n_0}k + (\epsilon - 1)\frac{2f^2}{n_0} \tag{25}$$

where $\frac{2f^2}{n_0}$ is the slope and $(\epsilon - 1)\frac{2f^2}{n_0}$ is the y-intercept, of the linear fit for the radii squared of the rings versus the number of the ring, k. The radii can be extracted using the best-fit curve of the rings,

$$Y = B - \sqrt{C^2 - (X - A)^2}, \tag{26}$$

where C^2 is the radius, A effects the placement on the X-axis, and B effects the placement on the Y-axis.

Difference between Wavelengths

To calculate how much the wavelength of the light emitted is shifted from the 546.1 nm emitted when there is no magnetic field, use Equation 8. Despite Equation 8 relating frequencies, they can written it in terms of wavelength. This results in

$$\Delta\lambda = \frac{c}{v_0 + \Delta v} - \frac{-c}{v_0} \tag{27}$$

$$\Delta\lambda = \frac{-c\Delta v}{v_0^2 - v_0\Delta v}, \tag{28}$$

where c is the speed of light, v_0 is the frequency when there is no magnetic field, and Δv is the change in frequencies between energy states.

Set Up and Procedure

Figure 4: Set Up of the experiment

The equipment for the experiment consist of a field probe, a power supply, a mercury lamp, an electromagnet, a lens/polarizer, a filter/Interferometer, a camera, and a track. In Figure 1, looking at the figure from left to right, the equipment is set up as the power supply, the electromagnet with the mercury lamp in the holder between the poles of the electromagnet, the lens/polarizer, the filter/Interferometer, and the camera. As the equipment is being set up, it is important to measure the placement and the height at which the equipment is set up so that it is easier to align the camera and so that in case something is moved or tampered with, the equipment could be set up the same as it was originally. The height of the center of the magnet is 18.5cm. This measurement is found by measuring from the table to the center of the metal screw on the side of the electromagnet. The height of the lens/polarizer is 22.5cm. This measurement is found by measuring from the table to the top of the lens/polarizer. The height of the filter/Interferometer is 22.5cm. This measurement is found by measuring from the table to the top of the filter/Interferometer. The height of the camera is 19.5cm. This measurement is found by measuring from the table to the center of the camera lens. In order to find the maximum magnetic field, the mercury lamp must removed and replaced by the field probe. The perpendicular field probe must be used to measure the maximum magnetic field because the electromagnet is perpendicular from the track. In order to reduce the uncertainty, the field probe must be rotated to find the maximum magnetic field. This measurements should be taken for 1A, 2A, 3A, 4A, and 5A.

Table 2: Magnetic field for each current.

Current (A)	Magnetic Field (mT)
1 ± 0.005	490 ± 5
2 ± 0.005	830 ± 5
3 ± 0.005	1015 ± 5
4 ± 0.005	1125 ± 5
5 ± 0.005	1215 ± 5

Experiment 1: Now, the mercury lamp must be placed back into the holder between the poles of the electromagnet, and then turn on the mercury lamp. The camera must be connected to the computer and use Logger Pro in order to observe the rings formed. In order to see a better image on logger pro, it might be helpful to place a black drape over the set up to block out any external light. Once the image on logger pro looks the best quality, set the lens/polarizer to 110 degrees so that the image has a sharper view. Record the image when there is no magnetic field, when the current is zero. After, another image must be recorded when the the current is at 5A. Experiment 2: Now, the lens/polarizer must be changed to 0 degrees. Then record the image when the current is at 5A. Experiment 3: For this part, the lens/polarizer must be removed. The record the image when the current is at 5A. While the lens/polarizer is removed, Remove the axial iron core plug from the electromagnet and rotate the electromagnet to 90 degrees, leaving it in the direction of the track. Then record the image when the current is at 5A.

Analysis and Results

3 Energy States

The first energy states that were seen were the three energy states that corresponded to the three middle transitions in Figure 1. Plotting the best fit of the ring's data points using Equation 26 resulted in Figure 5.

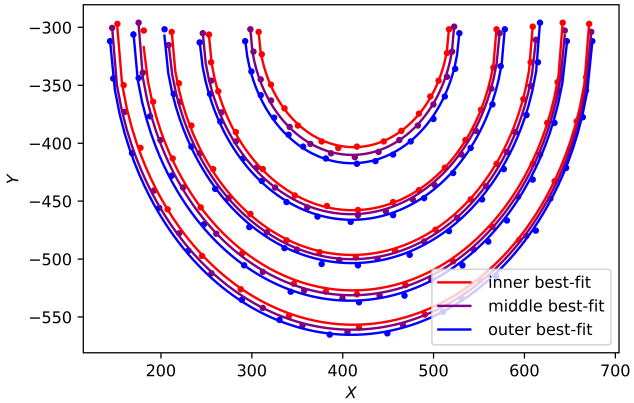

Figure 5: Best-fit curves for the rings at 3 energy states.

Taking the radii from the best-fit curves, they can be used to solve for ϵ by plotting the radii squared vs. the ring number, k. There were 3 states which correspond to the three energy states, where each k had five radii. The plot of the radii squared vs. k yielded a linear relationship, seen in Figure 6.

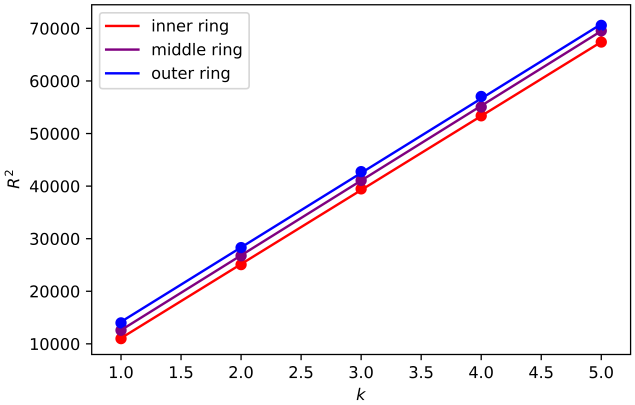

Figure 6: 3 energy states: plot of R^2 vs. k.

The linear fit's slope and intercept can be substituted into Equation 25 to find ϵ. Table 3 shows the ϵ value for each ring, k.

Table 3: The ring number and its corresponding ϵ.

k	ϵ
1	$0.781040 \pm 2.4 \times 10^{-5}$
2	$0.884373 \pm 3.6 \times 10^{-5}$
3	$0.984982 \pm 3.6 \times 10^{-5}$

With ϵ known, the Bohr magneton can be found since δ was found earlier in Table 3. Matching ϵ to its δ is seen in Table 4.

Table 4: ϵ with its δ pair.

ϵ num.	δ value
1	1/2
2	0
3	-1/2

Using Equations 22, 23, and 24, the slope of ϵ vs. δ can be used to find the Bohr magneton. The plot is seen in Figure 7.

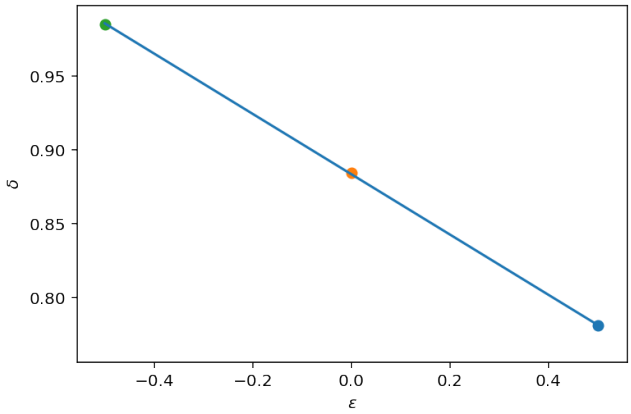

Figure 7: Plot of ϵ vs. δ. Slope = -0.204 $\pm$ 4.2×10^{-5} and y-intercept = 0.883 $\pm$ 1.8×10^{-5}

Substituting the slope into Equation 24, where $d = 0.001995 \pm 2 \times 10^{-6}$ m, $B = 1.180$ T, and $hc = 1.9864 \times 10^{-25}$ $\frac{\text{kg}*\text{m}^3}{\text{s}^2}$, resulted in a Bohr magneton of $8.616 \times 10^{-24} \pm 8.7 \times 10^{-27}$ J/T. This value is off from the accepted value of the Bohr magneton which is 9.274×10^{-24} J/T. It is expected when there are more energy states, the value of μ_B will become more accurate since there are more points of data.

6 Energy States

When the camera picks up 6 energy states, they corresponded to the $\Delta M_z = +1$ and -1 transitions in Figure 1. The analysis is similar to the 3 energy states where Equation 26 is used to find the radii. However, there are now 6 pairs of rings rather than just 3. The best-fit curves for the rings are in Figure 8. The inner most ring is $k = 1$ and goes through $k = 6$, and repeats. Each ring has 5 data points for a total of 30 individual rings.

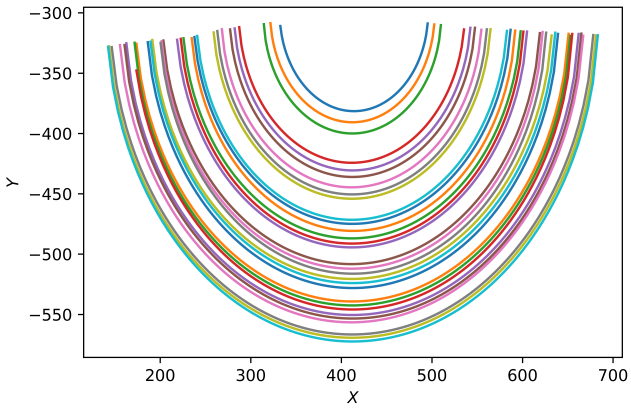

Figure 8: Best-fit curves for the rings at 6 energy states.

Using the radii provided from the best-fit curves, R^2 vs. k is plotted to find ϵ for each of the 6 states. The relationship is between the radii squared vs. k is linear which can be seen in Figure 9.

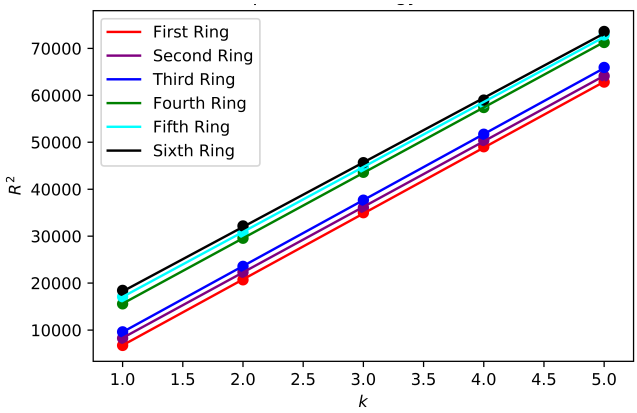

Figure 9: 6 energy states: plot of R^2 vs. k.

There is a gap between the third and fourth ring because these 6 energy states did not include the $\Delta M = 0$ transitions from Figure 1. The linear fit's slope and intercepts can be subsituted into Equation 5 to find ϵ for each of the 6 transitions. Table 5 contains the value of ϵ for each ring.

Table 5: The ring number and its corresponding ϵ.

k	ϵ
1	0.480037 ± 0.003
2	0.594344 ± 0.002
3	0.679508 ± 0.001
4	1.120143 ± 0.002
5	1.232006 ± 0.002
6	1.325633 ± 0.029

Pairing each ϵ to its appropriate δ is found in Table 6, where ϵ is plotted against δ to find the Bohr magneton.

Table 6: ϵ with its δ pair.

ϵ num.	δ value
1	2
2	3/2
3	1
4	-1
5	-3/2
6	-2

To extract the Bohr magneton plot δ vs. ϵ where the linear relationship can be found in Figure 10.

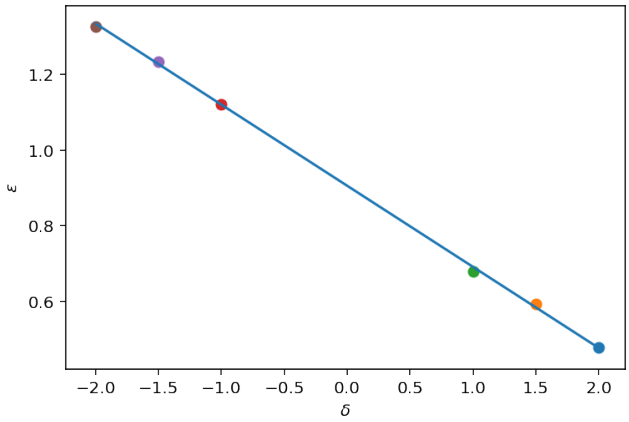

Figure 10: Plot of ϵ vs. δ. Slope = -0.214 $\pm$ 0.0005 and y-intercept of 0.905 $\pm$ 0.0007

Substituting the results from the linear fit into Equation 24 yields a Bohr magneton of $9.258 \times 10^{-24} \pm 9.07 \times 10^{-27}$ J/T. This value is extremely close to the accepted value of the Bohr magneton and is a great improvement over the value given from the 3 state analysis. Given the uncertainty in the calculated Bohr magneton from the 6 state analysis, it puts the value within 9.274×10^{-24} J/T.

9 Energy States

Following the same techniques and measurements in the previous two experiments, the Bohr magneton can be found for all 9 energy states described in Figure 1. The best fit curves to extract the radii is in Figure 11. The values of ϵ can be seen in Table 7.

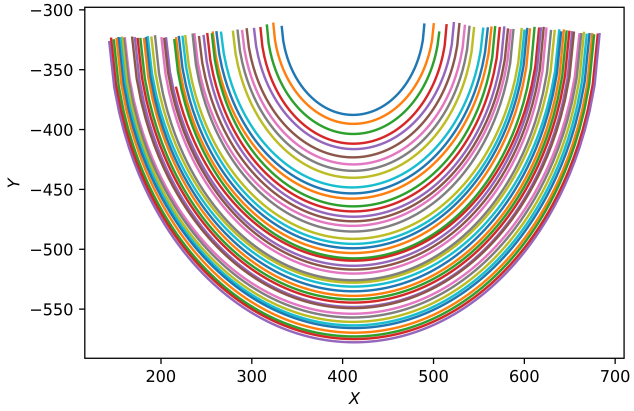

Figure 11: Best-fit curves fro the rings at 9 energy states

Using the plot of radii squared vs. k in Figure 12, provided Table 7 with ϵ for each ring.

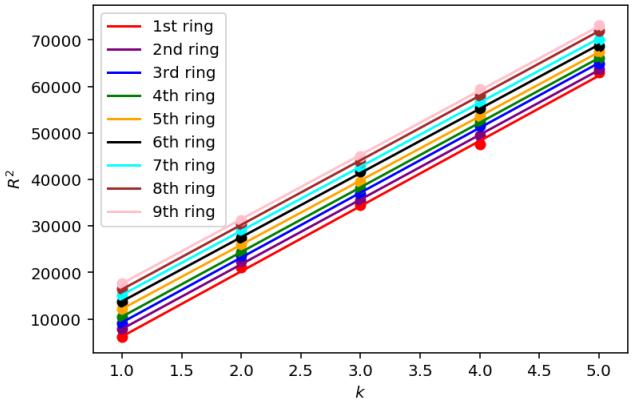

Figure 12: 9 energy states: plot of R^2 vs. k.

Table 7: The ring number and its corresponding ϵ.

k	ϵ
1	0.443685 ± 0.001
2	0.563763 ± 0.002
3	0.663759 ± 0.003
4	0.754531 ± 0.001
5	0.881168 ± 0.002
6	$.998889 \pm 0.001$
7	1.101501 ± 0.002
8	1.178845 ± 0.002
9	1.274902 ± 0.002

The pairings of ϵ and its quantum state, δ, can be seen in Table 8.

Table 8: ϵ with its δ pair.

ϵ num.	δ value
1	2
2	3/2
3	1
4	1/2
5	0
6	-1/2
7	-1
8	-3/2
9	-2

The slope of ϵ vs. δ is used to extract the Bohr magneton. Figure 13 is the linear fit.

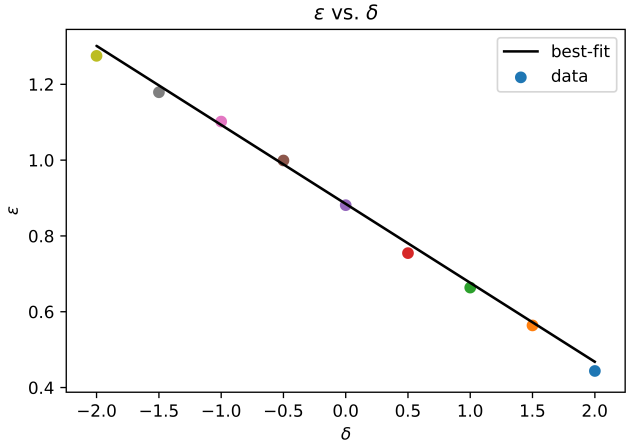

Figure 13: Plot of ϵ vs. δ. Slope = -0.208 $\pm$ 0.0003 and a y-intercept of 0.884 $\pm$ 0.0004

Taking the results from Figure 13 and substituting them into Equations 22, 23, and 24 yielded a Bohr magneton of $8.908 \times 10^{-24} \pm 8.9 \times 10^{-27}$ J/T. This value is not as close to the accepted value as the Bohr magneton from the 6 energy states, nonetheless, $8.908 \times 10^{-24} \pm 8.9 \times 10^{-27}$ J/T is a close approximation to 9.274×10^{-24} J/T.

Finding the Shifted Wavelengths

Using the 9 energy states from Figure 1, the shifted wavelengths from the 546.1 nm can be found. Using Equations 27 and 28, the difference between the wavelengths for each δ can be found. Knowing that v_0 is the frequency when there is no magnetic field, then $v_0 = 5.49 \times 10^{14}$ Hz when a wavelength to frequency conversion is used. Using Equation 8 to find each v, as well as the difference between v and v_0, allows for all the terms in Equation 28 to be known. Substituting everything into Equation 28 resulted in the wavelength difference which is found in Table 9.

Table 9: The difference in the wavelength for each energy transition for mercury.

Energy Transitions	$\Delta\lambda$
$+1 \rightarrow 0$	$-3.08 \times 10^{-11} \pm 5.46 \times 10^{-7}$ m
$0 \rightarrow$ -1	$-2.31 \times 10^{-11} \pm 5.46 \times 10^{-7}$ m
-1 $\rightarrow +2$	$-1.54 \times 10^{-11} \pm 5.46 \times 10^{-7}$ m
$+1 \rightarrow +1$	$-7.72 \times 10^{-12} \pm 5.46 \times 10^{-7}$ m
$0 \rightarrow 0$	0 m
-1 $\rightarrow$ -1	$7.72 \times 10^{-12} \pm 5.46 \times 10^{-7}$ m
$+1 \rightarrow +2$	$1.54 \times 10^{-11} \pm 5.46 \times 10^{-7}$ m
$0 \rightarrow +1$	$2.32 \times 10^{-11} \pm 5.46 \times 10^{-7}$ m
-1 $\rightarrow 0$	$3.09 \times 10^{-11} \pm 5.46 \times 10^{-7}$ m

These results made sense because it is expected that the greater the energy change then there will be a greater shift in the wavelengths.

Conclusion

This experiment allowed for the testing of the Zeeman effect which demonstrated the principal that atoms undergo transition in energies as they are exposed to a strong magnetic field. Through the use of interferometry as well as electro-magnetic principals, one can collect the necessary information to confirm the existence of the Zeeman effect, as well as solve for the fundamental constant of the Bohr magneton. These experiments yielded a Bohr mangneton of $8.616 \times 10^{-24} \pm 8.7 \times 10^{-27}$ J/T for 3 energy transitions, $9.258 \times 10^{-24} \pm 9.07 \times 10^{-27}$ J/T at 6 energy transitions, and $8.908 \times 10^{-24} \pm 8.9 \times 10^{-27}$ J/T at all 9 energy transitions, where the accepted value was 9.274×10^{-24} J/T. The determined Bohr magneton from the experiments in this lab are within 3% or less of the accepted value which supports that it is possible to solve for the Bohr magneton using the principals of interferometry and the Zeeman effect.